10.2478/v10170-010-0002-y

Archives of Control Sciences
Volume 20(LVI), 2010
No. 1, *pages 19–30*

Nonlinear response of a harmonically driven oscillator in magnetic field

PIOTR PRZYBYŁOWICZ and TOMASZ SZMIDT

The paper presents analysis of nonlinear response of a classical mechanical oscillator placed within a magnetic field and driven by a harmonic force. With an appropriate choice of control parameters, the system vibrates chaotically between different equilibrium positions. To prove this result, Lyapunov exponents have been calculated using the algorithm proposed by Rangarajan G., Habib S. and Ryne R. [18]. Moreover, the appropriate time series, phase portrait, Poincaré cross-section and power spectrum are given to support the conclusion.

Key words: nonlinear vibrations, oscillator, chaos, stability, magnetic damping

1. Introduction

The electromagnetic damping of a mechanical oscillator undergoing harmonic excitation was examined in [16] and [17]. It turned out that the damping can be efficient and the effect of magnetic hysteresis has a minor impact on reduction of vibration amplitude. Electromagnetic phenomena related to induction and hysteresis result in a nonlinear response of the oscillator. In this paper we prove that with an appropriate selection of control parameters, the system vibrates chaotically between different equilibrium positions.

The most powerful evidence of chaotic behavior is the highest positive Lyapunov exponent. There are several methods of calculating the highest exponent or even the whole Lyapunov spectrum. According to [3], the most popular one is the algorithm proposed by Wolf et al. [20]. It was used in investigations of chaotic behavior of many vibrating systems. Among them are analyzes of equations of the mathematical pendulum and Duffing oscillator subjected to harmonic excitation with random (white noise) frequency [11], Duffing equation with inertial excitation coming from an unbalanced rotor attached to the oscillator [7] and vibrations of a rotor supported by active magnetic bearings [12].

Wolf's algorithm is computationally expensive [1, 2, 3] and "not very robust" [10]. Therefore, new methods of computing Lyapunov exponents or determining chaos have

The Authors are with The Institute of Construction Machinery Engineering, Warsaw University of Technology, 02-524 Warsaw, Narbutta 84, Poland. E-mails: piotrp@ipbm.simr.pw.edu.pl, tomasz.szmidt@gmail.com

Received 30.09.2009. Revised 2.03.2010.

been developed. An analysis of wandering trajectories was proposed in [1] and applied to a harmonically forced Duffing oscillator [1] and to classical Masing and Bouc-Wen hysteretic oscillators [2]. Chaotic behaviour of linear vibrating systems with impacts was analyzed in [8] with a new algorithm earlier proposed by the authors (this method was further developed for systems without analytical solution between impacts, see [13]). Yet another algorithm was proposed in a paper concerned with the Van der Pol oscillator under parametric and external harmonic excitations [19] and free-vibrating undamped Lennard-Jones oscillator with impacts [21]. Worth mentioning is the analytical method of Melnikov functions, compared to Wolf's algorithm in the case of the Duffing system with nonlinear frictional damping and harmonic excitation [6].

The elegant method of computing the whole spectrum of Lyapunov exponents, which will be used in our work, was proposed by Rangarajan G., Habib S. and Ryne R. [18]. The authors derived a set of differential equations for Lyapunov exponents, which can be directly solved numerically. They tested the method with the classical harmonically driven Van der Pol oscillator and with the Lorenz system, in both cases getting agreement with numerical results obtained earlier through other methods.

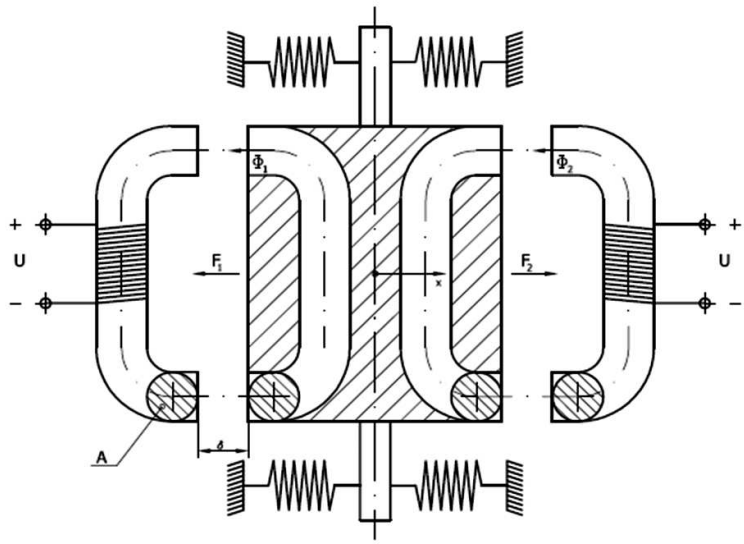

Figure 1. Examined system – armature elastically suspended between electromagnets.

2. Analyzed system

The system is very similar to the one examined by authors in [17]. Between two identical electromagnets, a mechanical harmonic oscillator of mass $m = 1.5$ [kg] is suspended on springs whose stiffness equals $k = 18000$ [N/m], see Fig. 1. Inside the os-

cillator there are steel cores embedded, which together with the electromagnets create a magnetic circuit with length $l = 200$ [mm] and diameter $2a = 3$ [mm]. Let us denote $A = \pi a^2$ the cross-section area of the core. Around each of the electromagnetic cores, $N = 320$ wire coils having electric resistance $R = 1.22\ \Omega$ are wound (copper with wire diameter 0.25 [mm]) to which a constant voltage $U = 7$ [V] is supplied. The gaps between the armature and electromagnets are: $z_1 = \delta + x$, $z_2 = \delta - x$, where $\delta = 1$ [mm], and $-\delta \leqslant x \leqslant \delta$ is a mechanically constrained displacement of the armature in the direction of the right-hand electromagnet. The parameter being changed in the investigations is the amplitude F_0 and frequency f of the harmonic force.

Electric conductivity of the steel cores (made of Si-Fe alloy, see [4]) amounts to $\sigma = 2 \cdot 10^6\ (\Omega\mathrm{m})^{-1}$. Its magnetic properties are described with the following 'trigonometric' primary magnetization curve

$$B = \varphi(H) = \operatorname{arctg}\left(H/400\right), \qquad H \geqslant 0. \tag{1}$$

The above $B - H$ curve and issuing curve of relative magnetic permeability $\mu = \mu(H) = \varphi(H)/(\mu_0 H)$, where $\mu_0 = 4\pi \cdot 10^{-7}$ [Tm/A] denotes magnetic permeability of vacuum, are presented in Fig. 2.

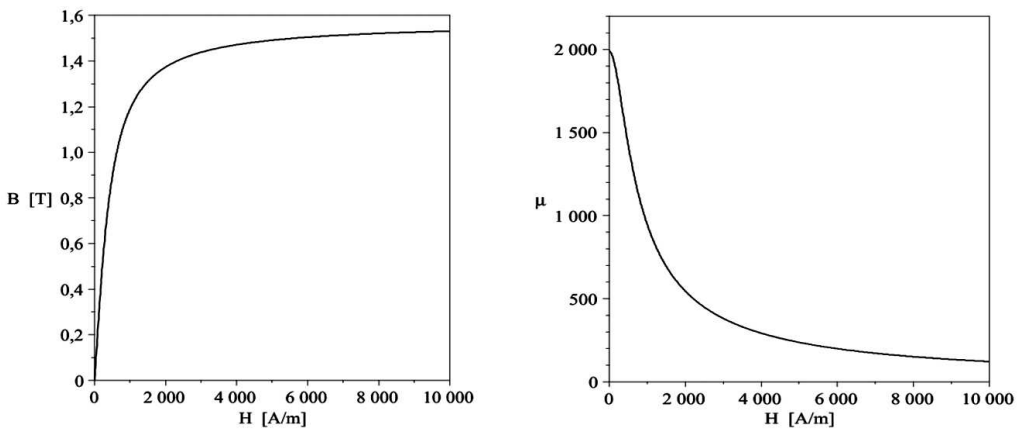

Figure 2. Primary magnetization curve and relative magnetic permeability of steel (according to eq. 1).

The shape of the real curve needs to be determined empirically. It depends not only on the content of alloy, but also on the thermal and mechanical treatment of the specific sample, which yields to different size and shape of grains and the crystallographic orientation. According to [4] and [5], the saturation of Si-Fe alloy $B_s \approx 1.5$ [T] is reached at

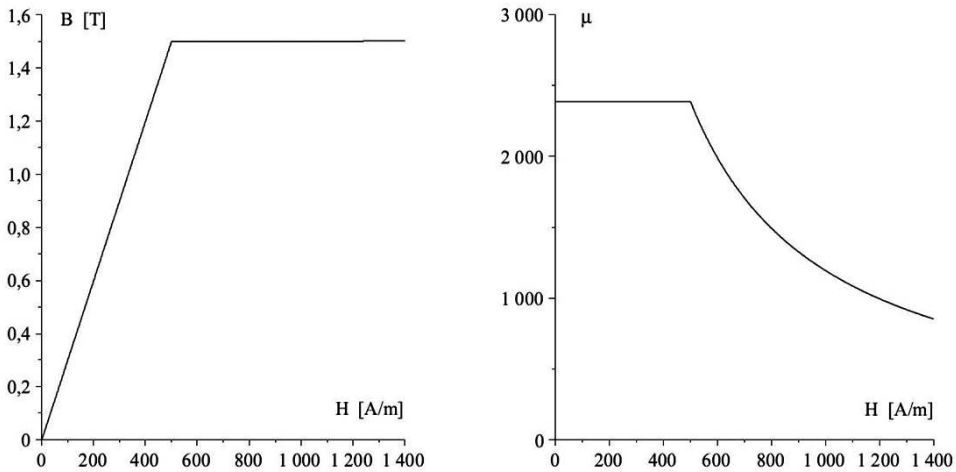

Figure 3. Primary magnetization curve and relative magnetic permeability of steel (according to [17]).

$H_s = 500 \ldots 5000$ [A/m][1], so the curve presented in Fig. 2 seems to be a good model of reality.

We changed the non-smooth bilinear curve used in [17] (see Fig. 3) and earlier in [9] for the one given by equation (1). The only reason for doing this was to make computations of Lyapunov exponents quicker. Numerical computations of damped vibrations showed that both curves that we have considered yield to similar results. What is most important here, is taking into considerations the effect of magnetic saturation, which leads to the appearance of new mechanical equilibrium points.

3. Dynamical equations

The dynamics for electric and magnetic circuits come from Maxwell's equations. A simple model of magnetic hysteresis by Bertotti is incorporated [4]. The detailed calculations presented in [17] yield the following equations for space-average magnetic induction in both rods $B_{1,2}$

$$\left(\frac{AN^2}{R} + \frac{1}{8} l\sigma a^2\right) \frac{\mathrm{d}B_{1,2}}{\mathrm{d}t} + 2\frac{(\delta \pm x)}{\mu_0} B_{1,2} + l\varphi^{-1}(B_{1,2}) = \frac{NU}{R}. \tag{2}$$

Derive now a formula for the magnetic force. Let us assume, for a while, the average induction in the core as a function of the gap size $B = B(z)$ exclusively. Shifting the

[1] According to [14], two definitions of saturation exist. We refer to practical and pretty imprecise definition of saturation, i.e. the maximum induction at which the $B-H$ curve starts to level-off. Theoretical definition of saturation $\lim_{H\to\infty}(B-\mu_0 H)$ is impractical, as it involves enormous magnetic field intensities, not encountered in our system.

oscillator away from the attracting electromagnet by a distance z, one accumulates in the magnetic field filling up the gap some potential energy of density

$$u(z) = \frac{B(z)^2}{2\mu_0}. \tag{3}$$

This expression is derived for an ideal solenoid, but it remains true for an arbitrary homogeneous magnetic field. Thus, the amount of energy accumulated in the gap of size z is

$$V(z) = \int_0^z u(y) A dy = \frac{A}{2\mu_0} \int_0^z B(y)^2 dy \tag{4}$$

and the magnetic force equals

$$F = 2\frac{dV}{dz} = \frac{A}{\mu_0} B^2. \tag{5}$$

Equation (5) is applicable to both electromagnets and the resultant magnetic force acting on the oscillator in the direction of the right-hand electromagnet equals

$$F_m = \frac{A}{\mu_0} \left(B_2^2 - B_1^2\right). \tag{6}$$

In Fig. 4, both magnetic F_m and elastic $F_e = kx$ forces are presented as functions of the oscillator displacement. The dependence of F_m on U is implicit. It can bee seen from eq. (2) – if one puts $dB_{1,2}/dt = 0$, then the static equation for $B_{1,2}$ is nonlinear with separate terms $B_{1,2}$ and $\mathrm{tg}(B_{1,2})$, therefore it has no explicit solution.

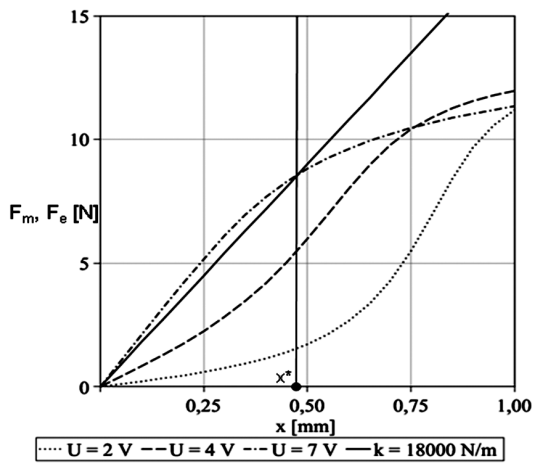

Figure 4. The magnetic F_m (eq. 6) and elastic $F_e = kx$ forces acting on the system.

The dynamics of the oscillator is governed by the coupled mechano-electromagnetic equations of motion, which have been derived using Newton's Second Law. The full system is described by the following set of nonlinear differential equations for the oscillator position x, see [17]

$$\begin{aligned} &m\ddot{x} = \frac{A}{\mu_0}\left(B_2^2 - B_1^2\right) - kx + F_0 \sin\left(2\pi f t\right) \\ &\left(\frac{AN^2}{R} + \frac{1}{8} l\sigma a^2\right) \frac{\mathrm{d}B_{1,2}}{\mathrm{d}t} + 2\frac{(\delta \pm x)}{\mu_0} B_{1,2} + l\varphi^{-1}\left(B_{1,2}\right) = \frac{NU}{R} \\ &x(0) = x_0, \quad \dot{x}(0) = v_0, \quad B_{1,2}(0) = \varphi\left(H_{01,2}\right) \end{aligned} \tag{7}$$

where $H_{01,2}$ is found from the implicit expression (index '1' refers to the left magnetic circuit, '2' – to the right one):

$$H_{01,2} = \frac{\frac{NU}{R}}{2\mu\left(H_{01,2}\right)\left(\delta \pm x_0\right) + l}. \tag{8}$$

4. Trajectories

The trajectories for $t = 0, 1/(32f), \ldots, 100$ [s] (sampling with frequency $32f$ and simulation length 100 [s]), and for $t = 0, 1/(4f), \ldots, 2000$ [s] have been generated using the Runge-Kutta-Fehlberg method applied to equations (7). The displacement of the oscillator for excitation frequency $f = 13$ [Hz] and sampling $32f$ is presented in Fig. 5.

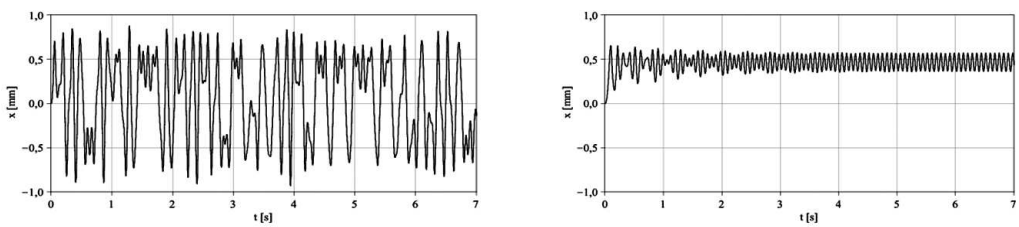

Figure 5. Displacement of the oscillator, amplitude $F_0 = 1.1$ [N] (left) and $F_0 = 0.3$ [N] (right), frequency $f = 13$ [Hz], sampling $32f$.

We can see that excitation amplitude $F_0 = 1.1$ [N] (left) results in chaotic vibrations of the oscillator. When we set $F_0 = 0.3$ [N] (right), the oscillator vibrates periodically around one of the mechanical equilibrium points $x^* \approx 0.48$ [mm] – the displacement for which elastic force equals magnetic one (see Fig. 4).

The power spectrum of the displacement, obtained for the same parameters and sampling, is presented in Fig. 6. We analyzed trajectories for time moments between 30 and

50 [s] to abandon the transient state at the beginning of simulation. Continuous spectrum on the left side (with one distinctive frequency of the excitation) is characteristic for chaotic systems. On the right side there is a spectrum with one peak corresponding to the excitation frequency and a small hump around the peak, which means that periodic vibrations are nearly harmonic.

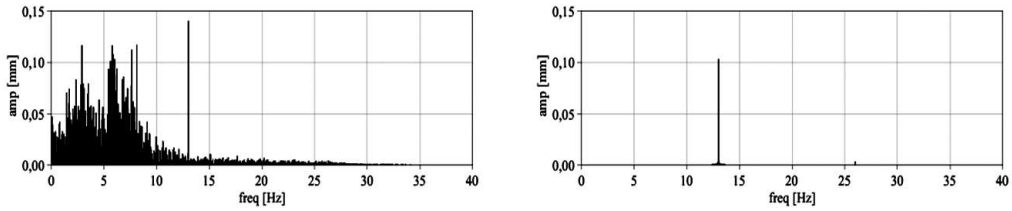

Figure 6. Power spectrum of displacement, amplitude $F_0 = 1.1$ [N] (left) and $F_0 = 0.3$ [N] (right), frequency $f = 13$ [Hz], sampling $32f$.

Similar conclusions arise when we observe the behavior of the system in 3-dimensional space (x, v, B_1), see Fig. 7. Here the trajectories calculated for time moments between 25 and 40 [s] were analyzed to omit the transient state at the beginning of simulation and make the chaotic attractor clear. On the left picture we can see that the attractor levels-off at the top of the box, which is due to the effect of magnetic saturation. Moreover, trajectories converge to the limit set, which probably has a fractional Hausdorff dimension (however computations of this dimension were not performed). Several other definitions of fractional dimension may be found in [15].

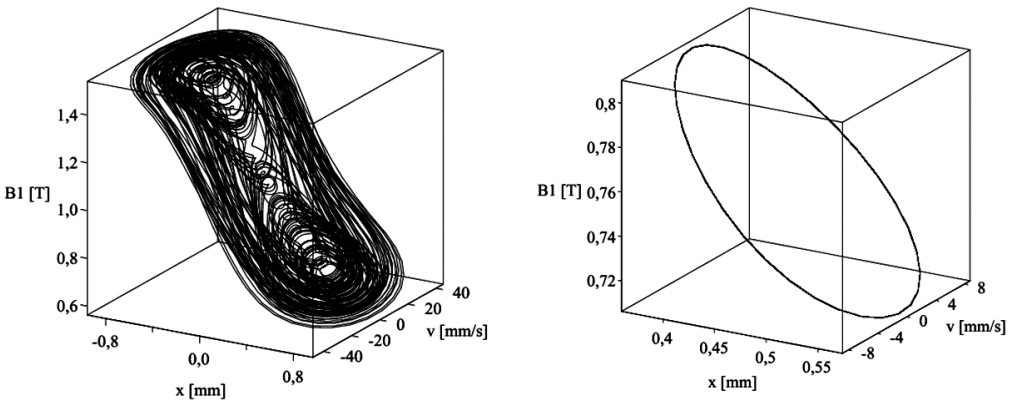

Figure 7. 3-d attractor in (x, v, B_1) space, amplitude $F_0 = 1.1$ [N] (left) and $F_0 = 0.3$ [N] (right), frequency $f = 13$ [Hz], sampling $32f$.

We close up qualitative analysis of the nonlinear behavior of the system with the Poincaré cross-sections on the $x - v$ plane for $t = 0, 1/f, \ldots, 2000$ [s], see Fig. 8.

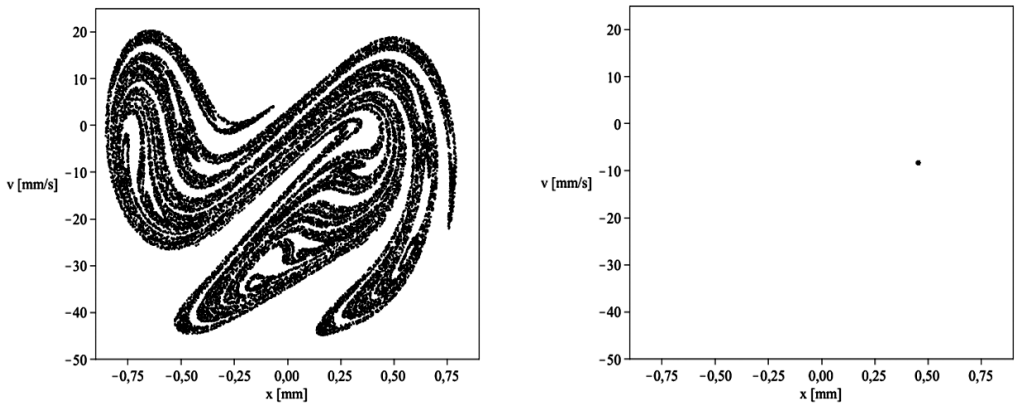

Figure 8. Poincaré cross-sections on the $x-v$ plane for $t = 0, 1/f, \ldots, 2000$ [s], amplitude $F_0 = 1.1$ [N] (left) and $F_0 = 0.3$ [N] (right), frequency $f = 13$ [Hz], sampling $4f$.

5. Lyapunov exponents

The most powerful evidence that a dynamical system exhibits chaotic behavior is the highest positive Lyapunov exponent. We calculated the whole spectrum of 4 Lyapunov exponents of the analyzed system using the algorithm proposed in [18], which will be described shortly here.

Dynamical system (7) is governed by the set of equations

$$\dot{z} = F(z,t) \tag{9}$$

where $z = (x, v, B_1, B_2)$. Suppose that the fiducial trajectory $z_0(t)$ is given for all t. Lyapunov exponents are strictly connected to the time evolution of deviations from the fiducial trajectory $Z(t) = z(t) - z_0(t)$. This evolution is obtained by linearization of (9) around z_0

$$\dot{Z} = DF_z(z_0,t) \cdot Z,$$

where $DF_z(z_0,t)$ denotes derivative of F with respect to variables z evaluated at z_0 and t. Integrating the above equations along the fiducial trajectory yields linear transformation $M(t)$, which turns the initial deviation Z_{in} into $Z(t)$

$$Z(t) = M(t) \cdot Z_{in}.$$

By differentiating this equation we obtain a differential expression for the matrix M

$$\dot{M} = DF_z \cdot M. \tag{10}$$

The Lyapunov exponents of (9) are equal to the logarithm of the eigenvalues of $\Lambda = \lim_{t\to\infty}(MM^T)^{1/2t}$.

Table 1. Lyapunov spectrum, frequency $f = 13$ [Hz], sampling $32f$

Lyapunov exp	λ_1	λ_2	λ_3	λ_4
$F_0 = 1.1$ [N]	11.7	-14.0	-3443	-10202
$F_0 = 0.3$ [N]	-0.6	-0.8	-3512	-8406

Instead of solving (10), the authors of the considered algorithm use linear algebra theorems to factorize the matrix M and obtain intrinsically well-behaved equations for the Lyapunov exponents and auxiliary variables. In our case, this approach leads to a set of 4 differential equations for system (7) together with 4 equations for Lyapunov exponents and 6 additional equations for angles. These 14 equations are given in an explicit form, however the equations for angles are especially complicated and cannot be included in the paper.

The trajectory for $t = 0, 1/(32f), \ldots, 100$ [s] has been generated using Runge-Kutta-Fehlberg integrator applied to 14 equations described above. The Lyapunov exponents converge to their true values when time goes to infinity – see Fig. 9 for convergence of the highest exponent.

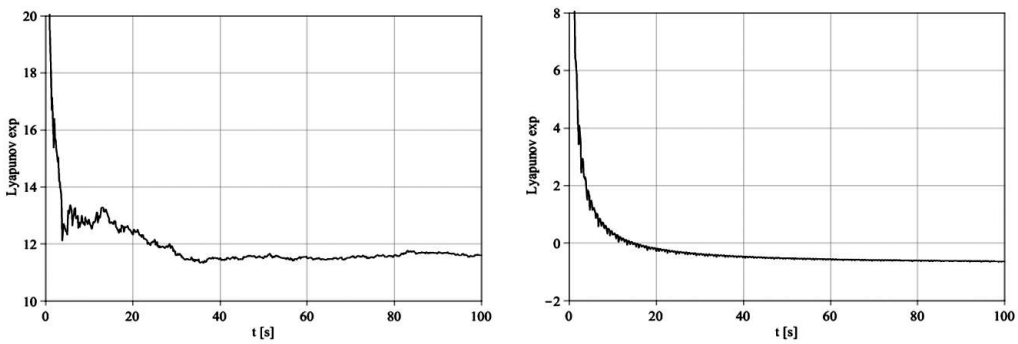

Figure 9. Convergence of the highest Lyapunov exponent, amplitude $F_0 = 1.1$ [N] (left) and $F_0 = 0.3$ [N] (right), frequency $f = 13$ [Hz], sampling $32f$.

The estimated values of the exponents have been calculated by taking averages for time moments $80 \leqslant t \leqslant 100$. The results are shown in Table 1.

From the beginning we assumed the amplitude of the excitation $F_0 = 1.1$ [N] for the chaotic behavior of the system and $F_0 = 0.3$ [N] for the periodic one. The dependence of the character of vibrations on the amplitude is presented in Fig. 10.

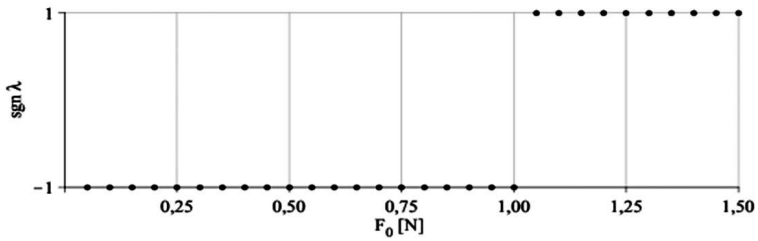

Figure 10. The sign of highest Lyapunov exponent, frequency $f = 13$ [Hz], sampling $32f$.

6. Concluding remarks

To sum up, we proved that in certain conditions, the analyzed system of an electromagnetically damped mechanical oscillator presents chaotic behavior. The algorithm proposed in [18] turned out to be efficient in computations of Lyapunov spectrum.

It is interesting if a real physical system would present similar chaotic behavior. We expect that several simplifying assumptions undertaken in the mathematical modeling of the system may have only minor influence on quantitative results, not qualitative ones.

In future research we will theoretically study a method of vibration damping by application of electromagnetic actuators in continuous systems, such as pipes conveying fluids or cantilever beams subjected to follower loads. Additionally, active control of the damping mechanism will be developed. Therefore, it is necessary to investigate dynamics of systems with magnetic actuators thoroughly, regardless of the fact whether the chaotic response in real conditions would appear or not.

References

[1] J. AWREJCEWICZ and L.P. DZYUBAK: Quantifying smooth and nonsmooth regular and chaotic dynamics. *Int. J. of Bifurcation and Chaos*, **15**(6), (2005), 2041-2055.

[2] J. AWREJCEWICZ and L.P. DZYUBAK: Influence of hysteretic dissipation on chaotic responses. *J. of Sound and Vibration*, **284** (2005), 513-519.

[3] J. AWREJCEWICZ and R. MOSDORF: Numerical analisis of chosen chaotic dynamical problems. WNT, Warsaw, 2003, (in Polish).

[4] G. BERTOTTI: Hysteresis in magnetism. Academic Press, San Diego, 1998.

[5] G. BIORCI and D. PESCETTI: Analytical theory of the behavior of ferromagnetic materials. *Il Nuovo Cimento*, **7**(6), (1958).

[6] M. BOROWIEC, G. LITAK and A. SYTA: Vibration of the duffing oscillator: Effect of fractional damping. *Shock and Vibration*, **14** (2007), 29-36.

[7] S.L.T. DE SOUZA, I.L. CALDAS, R.L. VIANA, J.M. BALTHAZAR and R.M.L.R.F. BRASIL: A simple feedback control for a chaotic oscillator with limited power supply. *J. of Sound and Vibration*, **299** (2007), 664-671.

[8] S.L.T DE SOUZA, I.L. CALDAS, R.L. VIANA, J.M. BALTHAZAR: Control and chaos for vibro-impact and non-ideal oscillators. *J. of Theoretical and Applied Mechanics*, **46**(3), (2008), 641-664.

[9] K. DZIEDZIC: Dynamic of rotors with active magnetic damping in bearings. PhD thesis , Warsaw University of Technology, 2005, (in Polish).

[10] H. GAN: Noise-induced chaos in duffing oscillator with double wells. *Nonlinear Dynamics*, **45** (2006), 305-317.

[11] H. HEIN and Ü. LEPIK: Response of nonlinear oscillators with random frequency of excitation, revisited. *J. of Sound and Vibration*, **301** (2007), 1040-1049.

[12] J.I. INAYAT-HUSSAIN: Chaos via torus breakdownin the vibration response of a rigid rotor supported by active magnetic bearings. *Chaos, Solitons and Fractals*, **31** (2007), 912-927.

[13] L. JIN, Q.-S. LU and E.H. TWIZZEL: A metod for calculating the spectrum of Lyapunov exponents by local maps in non-smooth impact vibrating systems. *J. of Sound and Vibration*, **298** (2006), 1019-1033.

[14] H.E. KNOEPFEL: Magnetic Fields. John Wiley & Sons, Inc., 2000.

[15] E. OTT: Chaos in dynamical systems. WNT, Warsaw, 1997, (in Polish).

[16] P.M. PRZYBYŁOWICZ and T. SZMIDT: Magnetic damping of harmonic oscillator vibration. *Modelowanie Inżynierskie*, **35** (2008), 101-106, (in Polish).

[17] P.M. PRZYBYŁOWICZ and T. SZMIDT: Electromagnetic damping of a mechanical harmonic oscillator with the effect of magnetic hysteresis. *J. of Theoretical and Applied Mechanics*, **47**(2), (2009), 259-273.

[18] G. RANGARAJAN, S. HABIB and R. RYNE: Lyapunov exponents without rescaling and reorthogonalization. *Physical Review Letters*, **80** (1998), 3747-3750.

[19] M. SIEWE SIEWE, F.M. MOUKAM KAKMENI, C. TCHAWOUA and P. WOAFO: Bifurcations and chaos in the triple-well Φ^6-Van der Pol oscillator driven by external and parametric excitations. *Physica A*, **357** (2005), 383-396.

[20] A. WOLF, J.B. SWIFT, H.L. SWINNEY and J.A. VASTANO: Determining Lyapunov exponents from a time series. *Physica D*, **16** (1985), 285-317.

[21] G. YANG, J. LU and A.C.J. LUO: On the computation of Lyapunov exponents for forced vibration of a Lennard-Jones oscillator. *Chaos, Solitons and Fractals*, **23** (2005), 833-841.